Bioactive Materials 6 (2021) 3924–3934

Contents lists available at ScienceDirect

Bioactive Materials

journal homepage: www.sciencedirect.com/journal/bioactive-materials

Supramolecular co-assembly of self-adjuvanting nanofibrious peptide hydrogel enhances cancer vaccination by activating MyD88-dependent NF-κB signaling pathway without inflammation

Qi Su [a], Huijuan Song [b,**], Pingsheng Huang [c,***], Chuangnian Zhang [c], Jing Yang [c], Deling Kong [d], Weiwei Wang [c,*]

[a] Department of Polymer Science and Engineering, School of Chemical Engineering and Technology, Collaborative Innovation Center of Chemical Science and Engineering (Tianjin), Tianjin University, Tianjin, 300072, China
[b] Institute of Radiation Medicine, Chinese Academy of Medical Sciences and Peking Union Medical College, Tianjin, 300192, China
[c] Tianjin Key Laboratory of Biomaterial Research, Institute of Biomedical Engineering, Chinese Academy of Medical Sciences and Peking Union Medical College, Tianjin, 300192, China
[d] State Key Laboratory of Medicinal Chemical Biology, College of Life Sciences, Nankai University, Tianjin, 300071, China

ARTICLE INFO

Keywords:
Cancer immunotherapy
Vaccination
Peptide
Co-assembly
Self-adjuvanting

ABSTRACT

Peptide vaccine targeting tumor-specific antigens is a promising cancer treatment regimen. However, peptide vaccines are commonly low-immunogenic, leading to suboptimal antitumor T-cell responses. Current peptide vaccination approaches are challenged by the variability of peptide physicochemical characters and vaccine formulations, flexibility, and the broad feasibility. Here, the supramolecular co-assembly of antigen epitope-conjugated peptides (ECPs) targeting CD8 or CD4 T-cell receptors was used to engineer a nanofibrious hydrogel vaccine platform. This approach provided precise and tunable loading of peptide antigens in nanofibers, which notably increased the antigen uptake, cross-presentation, and activation of dendritic cells (DCs). Immunization in mice indicated that the co-assembled peptide hydrogel did not induce local inflammation responses and elicited significantly promoted T-cell immunity by activating the MyD88-dependent NF-κB signaling pathway in DCs. Vaccination of mice using co-assembled peptide vaccine stimulated both enhanced CD8 and CD4 T cells against EG.7-OVA tumors without additional immunoadjuvants or delivery systems, and resulted in a more remarkable cancer immunotherapy efficacy, compared with free peptide vaccine or aluminum-adjuvanted peptide formulation. Altogether, peptide co-assembly demonstrated by three independent pairs of ECPs is a facile, customizable, and chemically defined approach for co-delivering peptide antigens in self-adjuvanting hydrogel vaccines that could induce stronger anticancer T-cell responses.

1. Introduction

Cancer immunotherapy that harnesses the immune system to fight tumor cells is transforming cancer treatment. Major immunotherapy regimens including immune checkpoint blockade, vaccination and adoptive cell transfer, have brought remarkable clinical benefits across a broad range of advanced cancers including melanoma, renal cell carcinoma and hematological malignancies [1–6]. Vaccination has long been used as an active approach to initiate the antitumor T-cell immunity for effective cancer immunotherapy [7,8]. Vaccine-primed cytotoxic T lymphocytes could specifically recognize, capture and eradicate cancer cells that adequately express tumor antigens (TAs), which would result in durable tumor inhibition and prolonged individual survival in both mice and humans. Beyond traditional cancer vaccines comprised of viral vectors, subunit proteins, or tumor lysates, synthetic peptides from antigenic epitopes are increasingly adopted as a new generation of TAs in the recent decade [9–11]. Highly specific peptide antigens have minimalistic and essential amino acid sequence, well-known

Peer review under responsibility of KeAi Communications Co., Ltd.
* Corresponding author.
** Corresponding author.
*** Corresponding author.
E-mail addresses: songhuijuan88@163.com (H. Song), sheng1989.2008@163.com (P. Huang), wwwangtj@163.com (W. Wang).

https://doi.org/10.1016/j.bioactmat.2021.03.041
Received 8 February 2021; Received in revised form 10 March 2021; Accepted 25 March 2021

mechanisms for inducing antigen-specific T-cell immunity, and superior safety. Furthermore, peptide antigens are easily manufactured in a low-cost and large-scale manner by solid phase peptide synthesis technology. However, currently available peptide vaccines are effective for a limited number of patients, even though in the context of personalized neoepitopes.

A major limitation to current peptide-based vaccine formulation is their insufficient efficacy of generating antigenic epitope-specific effector CD8 T cells in vivo. Recently, nano-, micro- or macro-engineering approaches have been developed to enhance both the strength and breadth of CD8 T-cell responses to peptide antigens [12–16]. A commonly used method is physically formulating peptide antigens and adjuvants into delivery systems including emulsions [17], liposomes [18], lipid nanodiscs [19], polymeric nanoparticles [20–22], and inorganic scaffolds [23], which were intentionally designed to improve the antigen presentation by dendritic cells (DCs) and thereby potentiate their immunogenicity potency. However, the peptide encapsulation, delivery and other formulation properties may be markedly different for each peptide antigen with distinct physico-chemical characters, leading to vaccine formulation variability. Moreover, the high-cost, complicated manufacture and potential safety concerns of delivery systems may limit the clinical translation of these technologies using as vaccination strategies. The formation of peptide vaccine depots at the injection site may deplete the autologous immune system that leads to suboptimal vaccine-specific CD8 T-cell immunity [24]. Alternatively, chemical conjugation of water-soluble peptide cargoes with hydrophobic segments including toll-like receptor agonists [25], lipids [19], dipalmitic acids [26], and self-assembling peptides [27–30], could trigger the self-assembly of nanoparticle, nanofiber or micelle structures. Antigens were also linked to a lipophilic albumin-binding tail to translate the “albumin hitchhiking” approach to molecular peptide vaccines [31]. These self-assembling vaccines provide main advantages that peptide loading is precisely and chemically defined, and immunoadjuvants or more peptide antigens could be covalently coupled to achieve co-delivery of dual components to DCs, which can greatly help to optimize T-cell priming. Whereas, these approaches were highly limited by the broad feasibility. The hydrophobic carriers could only chemically attach water-soluble peptide antigens and the content of an individual antigen could not be flexibly tuned in the vaccine, which was unfavorable to the modulation of vaccine components. In addition, the potential cellular signaling pathways that self-assembling peptide vaccines elicited T-cell responses remain to be demonstrated.

To address these challenges, we developed a distinctive peptide vaccine platform by the supramolecular co-assembly of two fully synthetic ECPs that ideally enabled the facile and precise loading of epitopes in the co-assembled hydrogel vaccine with defined nanofibrious structures (Scheme 1A). The co-assembly of vaccine was induced by simply mixing two ECPs in water in a modular, generalized and quantitative manner, which potentially overcame the manufacture and formulation limitations associated with current di- or multivalent peptide-based vaccines. Specially, epitopes targeting CD8 and CD4 T-cell receptors were used as model antigens based on the fact that the production of CD4 T cells could not only aid the priming of CD8 T cells, but also collaborate with them at the tumor site to maintain an effective antitumor response during immunotherapy [32,33]. Co-assembled hydrogel vaccine showed excellent self-adjuvanting property and greatly promoted the maturation of DCs and the following priming of T cells in vivo. In mice with established E. G7-OVA lymphoma tumors, the deployment of co-assembled peptide hydrogel as a vaccination strategy significantly increased the population of both CD4 and CD8 T cells at the tumor site (Scheme 1B), compared with vaccine formulations including the free or aluminum-adjuvanted epitope vaccine, thereby boosting the immunotherapy efficacy. Moreover, we demonstrate that the co-assembled peptide vaccine elicited T-cell immunity by activating the MyD88-dependent NF-κB signaling pathway in DCs (Scheme 1C) without inducing local inflammation responses.

2. Materials and methods

2.1. Materials

Ovalbumin (OVA) epitope peptides including MHCI-restricted epitope SIINFEKL (abbreviated as $OVA_{257-264}$) and MHCII-restricted epitope QAVHAAHAEINEAGR (abbreviated as $OVA_{323-336}$), CTL epitopes from melanoma-associated antigen MAGE including EADPTGHSY (abbreviated as MAGE-1) and FLWGPRALI (abbreviated as MAGE-2), carrier peptides including KWKAKAKAKWK (abbreviated as K peptide)

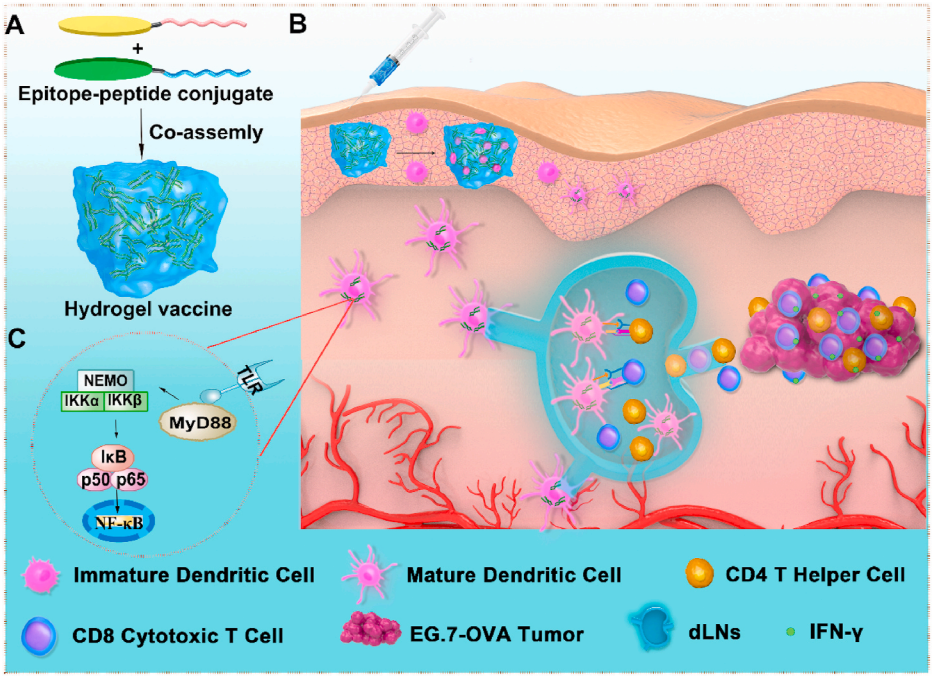

Scheme 1. The formation of co-assembled, self-adjuvanting peptide hydrogel vaccine with nanofiber structures and vaccination-mediated E. G7-OVA lymphoma immunotherapy. (A) Peptide conjugates chemically coupled with antigen epitopes were mixed in water to induce the spontaneous supramolecular co-assembly of nanofibrious hydrogel. (B) Subcutaneous vaccination of peptide hydrogel vaccines. Vaccines were uptaken by host DCs, processed and presented to naïve T cells, which differentiated into CD8 T and CD4 T helper cells. Effector CD8 cytotoxic T cells would capture and eradicate tumor cells along with the secretion of interferon-γ (IFN-γ). (C) The activation of MyD88-dependent NF-κB signaling pathway in DCs.

and EWEAEAEAEWE (abbreviated as E peptide), and epitope-conjugated peptides including KWKAKAKAKWKGGGSIINFEKL (abbreviated as K-$OVA_{257-264}$), KWKAKAKAKWKGGGEADPTGHSY (abbreviated as K-MAGE-1), EWEAEAEAEWEGGGQAVHAAHAEINEAGR (abbreviated as E-$OVA_{323-336}$), and EWEAEAEAEWEGGGFLWGPRALI (abbreviated as E-MAGE-2) were manufactured by solid-phase synthesis with yields ranged from 90 to 95%. The purity of all synthesized peptides was >95%. The peptides were used without further purification. Fluorescein isothiocyanate-labeled K-$OVA_{257-264}$ (K-$OVA_{257-264}$-FITC) and rhodamine B-labeled E-$OVA_{323-336}$ (E-$OVA_{323-336}$-RB) were provided by Bankpeptide biological technology co., LTD. Information for antibodies and adjuvants were supplemented in the Supporting Information.

2.2. Methods

2.2.1. Preparation and characterization of co-assembled peptide vaccines

To examine the peptide co-assembly, peptide pairs including K-$OVA_{257-264}$/E-$OVA_{323-336}$, K-MAGE-1/E-$OVA_{323-336}$, and K-$OVA_{257-264}$/E-MAGE-2 were dissolved in water at a mass ratio of 1:1 and the total peptide concentration was 10 mg/mL. To further study the co-assembly behavior, the structure morphologies of resulting aggregates were observed by TEM (JEM100CXII, JEOL). Z-average diameter (nm) of co-assembly peptides in aqueous solution were determined by DLS using Zetasizer Nano ZS (Malvern Instruments). The cytotoxicity of peptides against DC 2.4 cells was investigated by CCK-8 assay.

Synthetic peptides including K-$OVA_{257-264}$ and E-$OVA_{323-336}$, as a representative pair, were dissolved in water at a mass ratio of 1:1, while the total peptide concentration was varied in the range of 1–20 mg/mL. To further study the co-assembly behavior, the mass ratio between K-$OVA_{257-264}$ and E-$OVA_{323-336}$ was adjusted to 1:3 or 3:1. The self-assembly of each individual peptide was also investigated.

To assess the secondary structures of peptide assembly, the ellipticity of peptide aqueous solutions was measured by circular dichroism (CD) instrument (J-810, JASCO). Rheology analysis of hydrogels was examined by AR 2000ex rheometer (TA). The interior hydrogel microstructure was observed by scanning electron microscopy (SEM). To further test the peptide co-assembly, fluorescence resonance energy transfer (FRET) imaging was implemented. Experimental details were shown in the Supporting Information.

2.2.2. Cellular uptake of fluorescence-labeled peptide in bone marrow derived dendritic cells (BMDCs)

The isolation procedures of BMDCs from mice were provided in the Supporting Information. Cellular uptake of peptides by BMDCs was then investigated. FITC-K-$OVA_{257-264}$ was incubated with BMDCs for 1 h in the absence of serum. Cells were then washed three times with PBS and incubated with 50 nM LysoTracker® Red DND-99 (Invitrogen) for 30 min at 37 °C to stain lysosomes. Cells were washed, fixed with 4% paraformaldehyde, and stained by DAPI to label nuclei, which were observed by confocal laser scanning microscopy (CLSM, Leica DM6000) to analyze the intracellular location of peptides. FITC-positive cells were also quantificationally determined by flow cytometer (BD Accuri™ C6, BD Biosciences) at excitation wavelength of 492 nm and emission wavelength of 520 nm, respectively.

2.2.3. BMDCs maturation, antigen presentation and T cell cross-priming

BMDCs were incubated with free $OVA_{257-264}$, K-$OVA_{257-264}$ peptide in aqueous solution or co-assembled peptide hydrogel (abbreviated as gel vaccine) with a final epitope concentration of 500 nM. The maturation of BMDCs and T cell cross-priming were analyzed by flow cytometry. The secretion of IL-6, TNF-α, IFN-α and IFN-β by BMDCs was determined by ELISA kits. Furthermore, the expression of proteins including p38, Erk1/2, IκBα and p65 in BMDCs was analyzed by Western blot assay. Details for these experiments were provided in the Supporting Information.

2.2.4. The splenocyte proliferation and specific killing effect of CTLs

Briefly, the splenocyte proliferation was determined by co-culturing naïve T lymphocytes with mature DCs and the specific killing was examined by co-culturing activated T cells with EG.7-OVA tumor cells. The viability of T lymphocytes or tumor cells was determined by CCK-8 assay. Experimental details were shown in the Supporting Information.

2.2.5. Immunization in mice

Female C57BL/6 mice aged 6–8 weeks were received subcutaneous (s.c.) immunization with formulations including PBS, assembling peptides (E/K peptide), free epitope vaccine ($OVA_{257-264}$/$OVA_{323-336}$ mixture), and hydrogel vaccine composed of K-$OVA_{257-264}$ and E-$OVA_{323-336}$ at day 0, 7 and 21. The antigen dose was 200 μg per mouse. The spleen and lymph nodes were isolated and homogenized 7 days after the last immunization. T-cell expansion and mature DCs in the lymph nodes were analyzed by flow cytometry. Details for tissue processing and antibody staining were provided in the Supporting Information.

2.2.6. Footpad inflammation assay

Mice were anesthetized and received subcutaneous injection of 30 μL PBS, epitope vaccine in Alum adjuvant, or hydrogel vaccine in the hind footpad. The thickness of the hind feet was measured with a vernier caliper at the indicated points. Hematoxylin & eosin (H&E) staining was implemented to analyze the local inflammation. Experimental details for tissue processing could be found in the Supporting Information.

To assess the recruitment of cells and the release of inflammatory cytokines, mice were immunized with 100 μL above-mentioned formulations by peritoneal cavity injection. After 24 h, mice were sacrificed, injected with HBSS buffer (1 mL) into peritoneal cavity, and massaged for 30 times. Then the lavage fluid was collected and centrifuged (400 g, 5 min). The obtained cells analyzed by flow cytometry after antibody labelling. The cytokines in the collected supernatant were analyzed by ELISA.

2.2.7. Therapeutic efficacy and T-cell subpopulations in tumors

C57BL/6 J mice (6–8 weeks, female) were challenged with the subcutaneous injection of 1×10^6 EG.7-OVA cells into the left flank. Eight mice were included in each group. At day 7, mice were immunized subcutaneously with PBS, epitope vaccine, epitope vaccine with Alum adjuvant or co-assembled peptide hydrogel vaccine (antigen dose, 200 μg). The tumor size and mice body weight were measured every two days. To test the level of tumor infiltrating lymphocytes (TILs), the obtained cells were subjected to antibody labeling and detected by flow cytometry. Details for T-cell separation and antibody staining were provided in the Supporting Information.

2.3. Statistical analysis

Data were shown as means ± SDs. The statistically significant difference between two groups were analyzed by unpaired two-tailed student's *t*-test in Prism 6 (GraphPad Software). Multiple comparisons were performed by one-way ANOVA. $P < 0.05$ indicates statistically significant.

3. Results and discussion

3.1. Co-assembly and characterization of epitope-conjugated peptide vaccine

In the well-known cancer-immunity cycle [34], recognition and elimination of cancer cells by cytotoxic T lymphocytes is key for determining the efficacy of cancer immunotherapy. Synthetic long peptides comprising diverse CD8 T-cell epitopes have been studied as cancer vaccines that were delivered in liposome [35,36]. However, the composition of each peptide in the resultant vaccine was constant and immunoadjuvant was needed to boost vaccine immunogenicity.

Furthermore, this approach was not applicable for water-insoluble epitopes, which required the use of an additional delivery vehicle. Here, we developed an alternative approach for co-delivering peptide antigens in the vaccine formulation.

Supramolecular co-assembly of peptides was adopted as an effective strategy to construct a vaccine platform, in which the antigen loading and composition were both easily modulated and customized. Self-assembling peptide KWKAKAKAKWK and EWEAEAEAEWE were selected as carriers for epitope delivery. Epitopes from model antigen OVA and melanoma-associated antigen MAGE expressed in human melanoma [37,38], with different characters including solubility, charge and isoelectric point (PI), were used to examine the generalization of peptide co-assembly for vaccine manufacturing. The physicochemical properties for diverse epitopes were shown in Fig. 1A. The water-solubility of epitopes was indicated by GRAVY (grand average of hydropathicity), the smaller of GRAVY value the better water-solubility of epitopes. Each epitope was chemically conjugated to self-assembling peptide KWKAKAKAKWK (K peptide) or EWEAEAEAEWE (E peptide) by typical solid-phase synthesis method with a linker of amino acid sequence comprising three numbers of glycine (GGG). The chemical structures of peptides were shown in Fig. S1 and confirmed by HPLC and MS (Fig. S2-S5). Epitope-conjugated peptides (ECPs) would co-assemble via non-covalent intermolecular forces including electrostatic interaction among lysine (K) and glutamic acid (E), π-π stacking between tryptophan (W), hydrogen-bonding as well as hydrophobic interactions among water-insoluble epitopes [39–41]. The co-assembly of K-OVA$_{257-264}$/E-OVA$_{323-336}$, K-MAGE-1/E-OVA$_{323-336}$, K-OVA$_{257-264}$/E-MAGE-2, and K-MAGE-1/E-MAGE-2 as representative combinations of ECPs were tested by TEM. Fig. 1B showed simply mixing two ECPs allowed the spontaneous formation of nanofibers or nanoparticles in water, indicating the occurrence of peptide co-assembly, irrespective of the distinctive properties of individual epitope. Moreover, it seemed that

A

Epitopes	GRAVY	Charge	PI	Epitope-conjugated peptides	Abbreviation	Charge
SIINFEKL	0.49	0.0	7.00	KWKAKAKAKWKGGGSIINFEKL	K-OVA$_{257-264}$	6.00
FLWGPRALI	1.03	1.0	11.05	EWEAEAEAEWEGGGFLWGPRALI	E-MAGE-2	-5.00
EADPTGHSY	-1.47	-1.9	4.06	KWKAKAKAKWKGGGEADPTGHSY	K-MAGE-1	4.10
QAVHAAHAEINEAGR	-0.51	-0.8	6.03	EWEAEAEAEWEGGGQAVHAAHAEINEAGR	E-OVA$_{323-336}$	-6.80

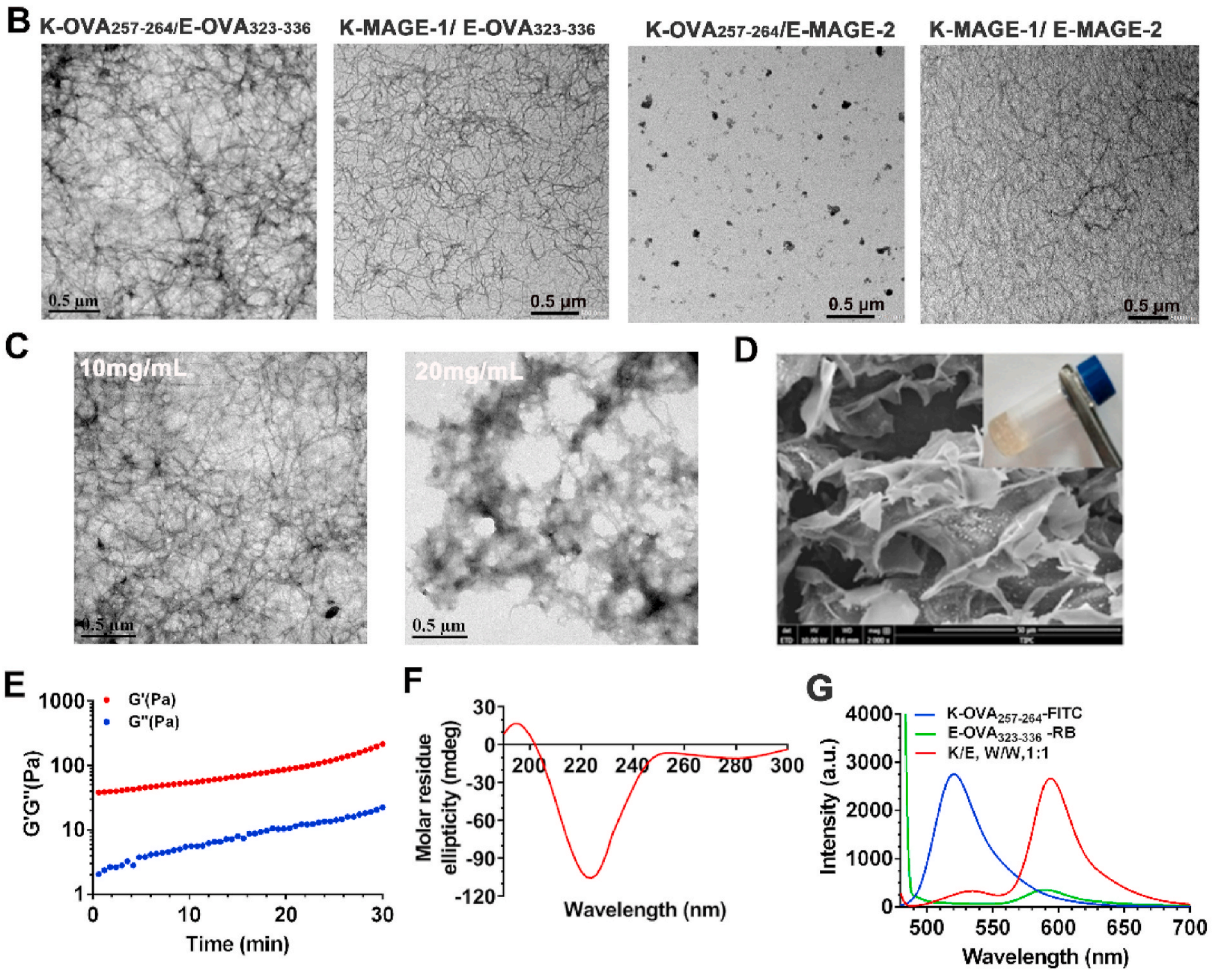

Fig. 1. Peptide co-assembly induced the formation of supramolecular vaccine with defined nanostructure. (A) The physicochemical properties of epitopes and epitope-conjugated peptides. GRAVY, grand average of hydropathicity. (B) Representative TEM images for co-assemblies of dual ECPs. (C) K-OVA$_{257-264}$/E-OVA$_{323-336}$ co-assemblies (concentration, 10 or 20 mg/mL). (D) Representative SEM image for K-OVA$_{257-264}$/E-OVA$_{323-336}$ co-assembly at a concentration of 20 mg/mL. Digital photograph for hydrogel was inserted. (E) Time sweep of co-assembled K-OVA$_{257-264}$/E-OVA$_{323-336}$ hydrogel. G′, storage modulus; G″, loss modulus. (F) Circular dichroism (CD) spectra of co-assembled K-OVA$_{257-264}$/E-OVA$_{323-336}$ nanofibers. (G) Representative emission spectra of free K-OVA$_{257-264}$-FITC, E-OVA$_{323-336}$-RB and the mixture of K-OVA$_{257-264}$/E-OVA$_{323-336}$ (weight ratio, 1/1; excitation wavelength, 465 nm).

the co-assembly of dual ECPs containing dual water-soluble epitopes or one water-insoluble epitope resulted in the assembly of nanofibers, while that for two water-insoluble epitopes were nanoparticles. This phenomenon may be attributed to the strong hydrophobic interaction that could induce the formation of nanoparticles.

Then, using K-$OVA_{257-264}$/E-$OVA_{323-336}$ as a model pair, the peptide co-assembly was further investigated. MHCI-restricted $OVA_{257-264}$ and MHCII-restricted $OVA_{323-336}$ peptide were with high-affinity to $CD8^+$ and $CD4^+$ T-cell, respectively. K-$OVA_{257-264}$ or E-$OVA_{323-336}$ alone self-assembled into nanoparticles in aqueous solution as indicated by TEM and DLS (concentration, 1 mg/mL; Fig. S6A, S6B, S7). Whereas, when the two were mixed with a mass ratio of 1/1 and at a total peptide concentration of 1 or 10 mg/mL, tangled nanofibers (Fig. 1C) were generated in solution. If the peptide concentration was further increased to 20 mg/mL, the density of nanofibers was significantly increased and highly overlapped nanofibrous structures were observed. Meanwhile, a hydrogel was spontaneously formed (Fig. 1D) with porous and three-dimensional interpenetrating networks, when peptides were dissolved in aqueous solution. Rheological analysis (Fig. 1E) confirmed the hydrogel formation as indicated by the fact that during the time sweep within 30 min, the value of storage modulus G′ is greater than that of the loss modulus G″, when the feeding mass ratio was 1/1 and 3/1 or 1/3 (Fig. S8). The strength of hydrogel was weak since there were only non-valent intermolecular forces for peptide co-assembly. Moreover, the obtained hydrogel was neither temperature-sensitive nor self-standing. By varying the feeding mass ratio for peptide co-assembly, the content of $OVA_{257-264}$ in the vaccine could be precisely and easily tuned in the magnitude from 8.8% to 28.1%. This data suggested the modular co-assembly of two ECPs could be facilely modulated by easily tuning the peptide mass ratio or adjusting the peptide concentration, to obtain a solution or hydrogel vaccine.

Then, the secondary structure of peptide in aqueous solution was explored by circular dichroism (CD), which is an important factor that determines the assembly behavior. In the CD spectrum (Fig. 1F, peptide concentration, 1 mg/mL), a positive band at 195 nm and a broad, strong negative band at 205–240 nm were observed, indicating that the secondary structure was dominated by β-sheets with partial α-helical conformation. The red-shift of β-sheet band from the standard 216 nm–225 nm demonstrated the formation of peptide aggregates in water, inducing the change in the polar microenvironment around peptide bonds and the n–π^* transition of peptide bonds [42,43]. However, K-$OVA_{257-264}$ or E-$OVA_{323-336}$ alone showed a typical β-sheet or random coil conformation (Fig. S9), respectively.

To further study the co-assembly of K-$OVA_{257-264}$ and E-$OVA_{323-336}$, fluorescence energy resonance transfer (FRET) imaging, a straightforward tool to detect the nanoscale distance (<10 nm) among assembling molecules, was performed. K-$OVA_{257-264}$ and E-$OVA_{323-336}$ were chemically labeled by fluorescein isothiocyanate (FITC) and rhodamine B (RB), respectively, which was proven an effective FRET pair [44]. Fig. 1G shows that at an excitation wavelength of 465 nm, a strong fluorescence peak at 530 nm that is characteristic emission of FITC was observed for K-$OVA_{257-264}$-FITC, while a quite weak fluorescence peak at 595 nm assigned to characteristic emission of RB was found for E-$OVA_{323-336}$-RB. However, when K-$OVA_{257-264}$-FITC and E-$OVA_{323-336}$-RB were mixed at a weight ratio of 1/1, the fluorescence at 530 nm was dramatically diminished while that at 595 nm was significantly increased, indicating the occurrence of FRET and the co-assembly of two peptides. The FRET efficiency was 89.1%. These data indicate that the spontaneous co-assembly of two distinct ECPs is a powerful strategy to manufacture divalent peptide vaccines with nanostructures. By facilely tuning the feeding mass ratio between peptides or the peptide concentration, nanofibrious solution or hydrogel vaccine could be produced. In addition, such a modular co-assembly manner provides a novel approach to precisely titrate the epitope content in vaccine.

3.2. Co-assembled peptide hydrogel vaccine enhanced antigen presentation and cross-priming of T cells

To produce a successful peptide vaccine composed of adequately expressed antigens, effective activation of antigen-presenting cells (APCs) is a crucial step to initiate T-cell priming [45]. Therefore, epitope peptides must be successfully delivered to APCs, processed and presented in an efficient way to engage the activation of naïve T cells. First, the cytotoxicity of each peptide against DC 2.4 cells was investigated by CCK-8 assay and results (Fig. S10) showed peptide was non-toxic when the concentration was lower than 2000 or 1000 nM. We then examined the peptide self-assembly in facilitating antigen uptake by DCs and localization in DCs by comparing native $OVA_{257-264}$ with self-assembling K-$OVA_{257-264}$. Lysine residue in $OVA_{257-264}$ was modified with FITC, which can retain its binding capacity to H-$2K^b$ [46], to obtain $OVA_{257-264}$-FITC and K-$OVA_{257-264}$-FITC, respectively. As shown in Fig. 2A, BMDCs incubated with free $OVA_{257-264}$-FITC displayed weak fluorescence signals of peptides in the lysosome, while cells treated with K-$OVA_{257-264}$ showed much stronger FITC signals, suggesting a higher level of peptide endocytosis by BMDCs. Moreover, peptides were mostly localized in the cytoplasm, but not in endosomes or lysosomes, for both free epitopes and self-assembling K-$OVA_{257-264}$ vaccine. Fig. 2B showed that a notably higher percentage of FITC-positive DCs was detected with K-$OVA_{257-264}$ treatment, in comparison with free peptide. These data confirmed that self-assembling K-$OVA_{257-264}$ could result in superior antigen uptake, enabling remarkably better activation of DCs compared with naked peptide, as indicated by a significantly higher ratio of $CD86^+$ DCs (Fig. 2C).

Next, antigen cross-presentation was examined by detecting the level of SIINKFEL displaying. DCs were stained by 25-D1.16 monoclonal antibody against SIINFEKL/H-$2K^b$ complexes. BMDCs pulsed with K-$OVA_{257-264}$ achieved ~5−fold increase in the efficiency of SIINFEKL presentation over DCs stimulated with free peptide (Fig. 2D). Co-assembled hydrogel vaccine further augmented the efficacy of SIINFEKL cross-presentation. These data suggested self-assembling K-$OVA_{257-264}$ vaccine or co-assembled gel vaccine could obviously enhance the antigen presentation by DCs. To assess T-cell cross-priming, BMDCs pre-treated with free antigen peptides, K-$OVA_{257-264}$ or co-assembled gel vaccine for 24 h, were cultured with B3Z T-cells that were SIINFEKL-specific and H-$2K^b$-restricted. Fig. 2E indicated that BMDCs pulsed with self-assembling K-$OVA_{257-264}$ or co-assembled gel vaccine robustly promoted B3Z T-cell activation as characterized by significantly higher fluorescence at 405 nm, whereas free SIINFEKL peptide induced minimal B3Z T-cell activation. Furthermore, co-assembled peptide vaccine resulted in superior T-cell priming over self-assembled peptide vaccine.

Then, the specific killing to tumor cells by CTLs induced by co-assembled peptide vaccine was examined. Mature DCs were incubated with naïve T-lymphocytes (Tn) isolated from the spleen for 72 h to test the proliferation of Tn. Fig. 2F shows that co-assembled peptide vaccine significantly facilitated the proliferation of splenocytes by 2-folds, compared with PBS or free epitope vaccine, indicating an effective cross-priming of $CD8\alpha^+$ T cells. Afterward, activated CTLs and E.G7-OVA tumor cells were co-cultured for 24 h to investigate the initiation of specific lysis of tumor cells by CTLs. Fig. 2G shows that the killing rate of T lymphocytes activated by co-assembled peptide vaccine-stimulated DCs on tumor cells reached 50% with a ratio of effector T lymphocytes to E.G7-OVA cells at 10:1, which was significantly higher than free epitope vaccine. These data demonstrated co-assembled peptide vaccine could potently activate DCs, which then presented peptide antigens to T cells, and provoke CTL response in vitro.

3.3. Co-assembled peptide vaccine elicited T-cell responses without inducing inflammation

Commonly, after vaccine administration antigens are uptaken,

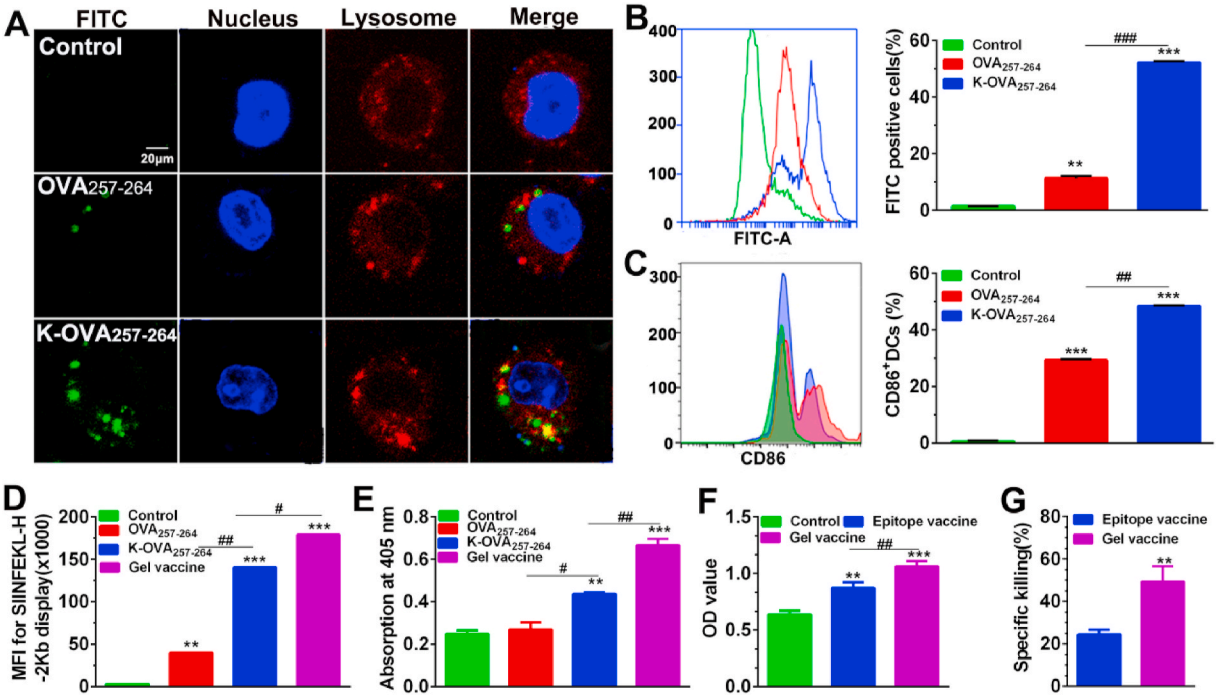

Fig. 2. Self-assembled and co-assembled peptide vaccine promoted antigen cross-presentation and T-cell priming in vitro. (A) Cellular uptake and intracellular localization of peptide epitopes observed by CLSM. (B) Quantitative analysis of peptide uptake by flow cytometry. (C) The percentage of $CD86^+$ BMDCs after incubation with $OVA_{257-264}$ or K-$OVA_{257-264}$ for 24 h. (D) The SIINFEKL presentation measured by flow cytometry. (E) Antigen cross-presentation by BMDCs incubated with various vaccine formulations. (F) The proliferation of splenocytes stimulated by mature DCs. (G) The specific CTL killing efficiency against E.G7-OVA cells in vitro. Data are shown as mean ± SDs (n = 3). $^*P < 0.05$, $^{**}P < 0.01$ and $^{***}P < 0.001$, versus the control; $^{\#}P < 0.05$ and $^{\#\#}P < 0.01$ and $^{\#\#}P < 0.01$, between the indicated groups.

processed and then transported to draining lymph nodes (dLNs) by host DCs, during which DCs becomes mature. Immune responses would be initiated in dLNs. To assess the activation of T-cell responses, mice were immunized with soluble carrier peptides, epitope vaccine, or co-assembled hydrogel vaccine for triple times. T cells and DCs in LNs were analyzed by flow cytometry after antibody staining. Fig. 3A shows that the percentage of $CD11c^+MHCII^+$ DCs was significantly increased with the immunization of hydrogel vaccine, compared to the mixture of free peptide epitopes, suggesting the extensive activation and maturation of host DCs in LNs. Further, immunization with the hydrogel vaccine resulted in significantly higher ratios of both $CD8^+$ and $CD4^+$ T cells in total $CD3^+$ T cells, compared with the free peptide vaccine, demonstrating a robust T-cell responses both in dLNs (Fig. 3B) and spleens (Fig. S11). Consequently, co-assembled hydrogel vaccine could promote the immunogenicity of peptide antigens and elicit a stronger T-cell responses over the mixture of free peptides.

A popular design strategy for modern peptide vaccines has focused on the use of immunoadjuvants to improve antigen immunogenicity [47]. Commonly used immunoadjuvants including Alum, MF59 and CFA, can initiate the adaptive immune response by targeting cells in the innate immune system [48–50], but generally induce inflammation at the injection site characterized by the secretion of inflammatory chemokines including MCP-1a/CCL2 and KC/CXCL1, as well as cytokines such as IL-1b, IL-5, IL-6, and G-CSF. A recent study of three Alum-based

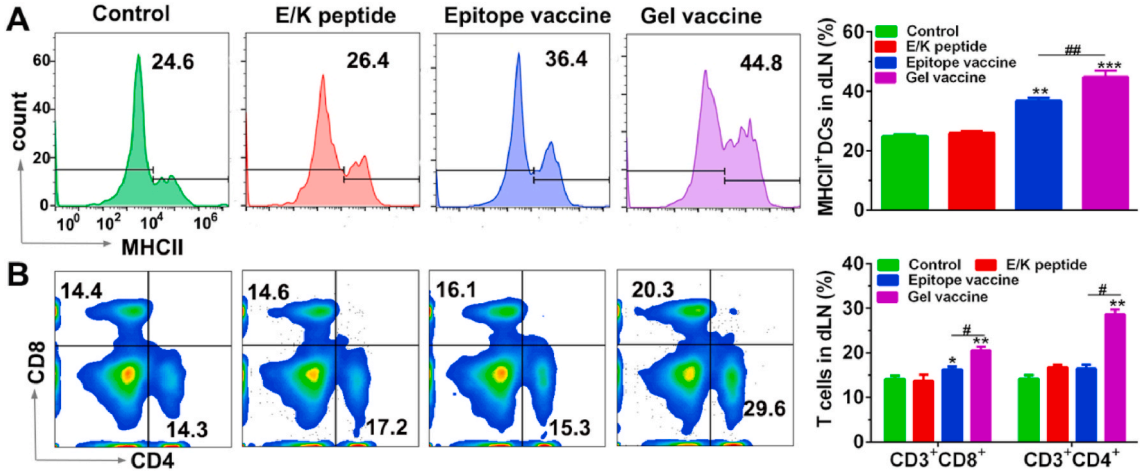

Fig. 3. Co-assembled peptide vaccine elicited superior T-cell responses than naked peptide vaccine in mice. (A) The percentage of $MHCII^+CD11c^+$ DCs in dLNs. Epitope vaccine, $OVA_{257-264}/OVA_{323-336}$; hydrogel vaccine, K-$OVA_{257-264}$/E-$OVA_{323-336}$. Data are shown as mean ± SDs (n = 5). (B) The ratio of $CD3^+CD8^+$ and $CD3^+CD4^+$ T cells in dLNs analyzed by flow cytometry. $^*P < 0.05$, $^{**}P < 0.01$ and $^{***}P < 0.001$, versus the control; $^{\#}P < 0.05$, between the indicated groups.

vaccine formulations proved that the immunogenicity correlated with the inflammation levels [51], complicating the design of peptide vaccines containing adjuvants. In this context, whether the immune responses elicited by co-assembled peptide vaccine were accompanied with inflammation was examined using peptide vaccine adjuvanted by FDA-approved Alum adjuvant, as a positive control. The inflammatory response was first detected by histopathology after footpad injection of vaccines. Fig. 4A indicates that the color and thickness of the gel vaccine-immunized footpads were similar to the non-immunized contralateral footpad, while the Alum-adjuvanted vaccine-immunized footpads turned red and swelled to 190% of their normal thickness, and the swelling exceeded one week (Fig. 4B). The swelling of footpads from mice received injection with gel vaccine was much lower than these treated by epitope vaccine. In histological cross-sections (Fig. 4C) of skin tissues stained by H&E at day 7, there was no difference between the gel vaccine-immunized footpads and the unimmunized controls, while epitope vaccine in Alum-immunized footpads mainly showed acute inflammation and muscle cell death in the subcutaneous muscle layer. Thus, gel vaccine resulted in dramatically diminished local inflammatory response compared with peptide vaccine in Alum.

Next, we examined the recruitment of host cells and the production of inflammatory cytokines after intraperitoneal (i.p.) injection, which can facilitate sampling and raise a similar or higher response profile to or than subcutaneous (s.c.) injection [52,53]. After injection for 24 h, cells including macrophages and monocytes (Fig. 4D) recruited by gel vaccine immunization in peritoneal lavage fluid was comparable with these in PBS-immunized mice. However, the recruitment of neutrophils by gel vaccine was also increased in comparison with that in control, because neutrophils are one of the first immune cells in the innate immune system that are recruited to the injury or infection site. Gel vaccine also induced similar levels of cytokines (Fig. 4E) including granulocyte colony-stimulating factor (G-CSF), monocyte chemotactic protein-1 (MCP-1), macrophage colony-stimulating factor (M-CSF), and interleukin-6 (IL-6) to PBS treatment, indicating the absence of inflammation. In contrast, immunization with Alum-adjuvanted epitope vaccine could recruit a large number of inflammatory cells in enterocoelia and caused notably higher levels of inflammatory chemokines and cytokines, compared with PBS or gel vaccine treatment. These data suggested that co-assembled peptide vaccine could stimulate the T-cell responses through a non-inflammatory pathway, which is distinct from peptide vaccine comprising Alum adjuvant.

3.4. Co-assembled peptide vaccine effectively activated the MyD88-dependent NF-κB signaling pathway in DCs

Self-assembling peptide vaccines have shown promising self-adjuvanting property [54–56], which could increase the efficacy of DCs maturation and cross-presentation of peptide antigens. However, the mechanism accounted for the self-adjuvanticity is still largely unknown. It has been reported that NLR family pyrin domain-containing protein 3 (NLRP3) inflammasome dominated the adjuvanticity of Alum [57], while MF59 and major Toll-like receptor (TLR) agonists were independent of NLRP3 inflammasome but required the adaptor myeloid differentiation primary response protein 88 (MyD88) [58]. TLR signaling pathways arise from intracytoplasmic TIR domains, including MyD88, TIRAP (TIR domain containing adaptor protein), and TRIF (TIR-domain-containing adapter-inducing interferon-β) adaptors [59]. MyD88 plays a crucial role in recruiting IL-1 receptor-associated kinase (IRAK) to TLRs. IRAK activated by phosphorylation then binds to TRAF6, which leads to the activation of two different downstream signaling pathways, and ultimately the activation of JNK (Jun N-terminal kinase) and NF-κB (nuclear factor kappa B).

In this context, the contribution of MyD88 to the elicitation of T-cell immunity elicited by co-assembled peptide vaccine in mice was first explored. The antigen presentation and activation of BMDCs from WT (wild type) and MyD88−/− knockout mice were compared. Fig. 5A demonstrated co-assembled hydrogel vaccine resulted in an eight-fold increase in antigen cross-presentation over the other two groups in WT mice, but the cross-presentation was dramatically decreased in DCs from MyD88−/− mice. Meanwhile, the expression of costimulatory molecule CD40 (Fig. 5B), and the production of IL-6 (Fig. 5C) and IFN-β (Fig. 5D) were all significantly downregulated in MyD88-lacking DCs, while the secretion of IFN-α (Fig. S12A) and TNF-α (Fig. S12B) were not affected. These data suggested that MyD88 was required for the activation of BMDCs and antigen cross-presentation by co-assembled peptide vaccine.

Afterward, the activation of NF-κB signaling pathway was examined to further clarify the molecular mechanism in the MyD88 downstream

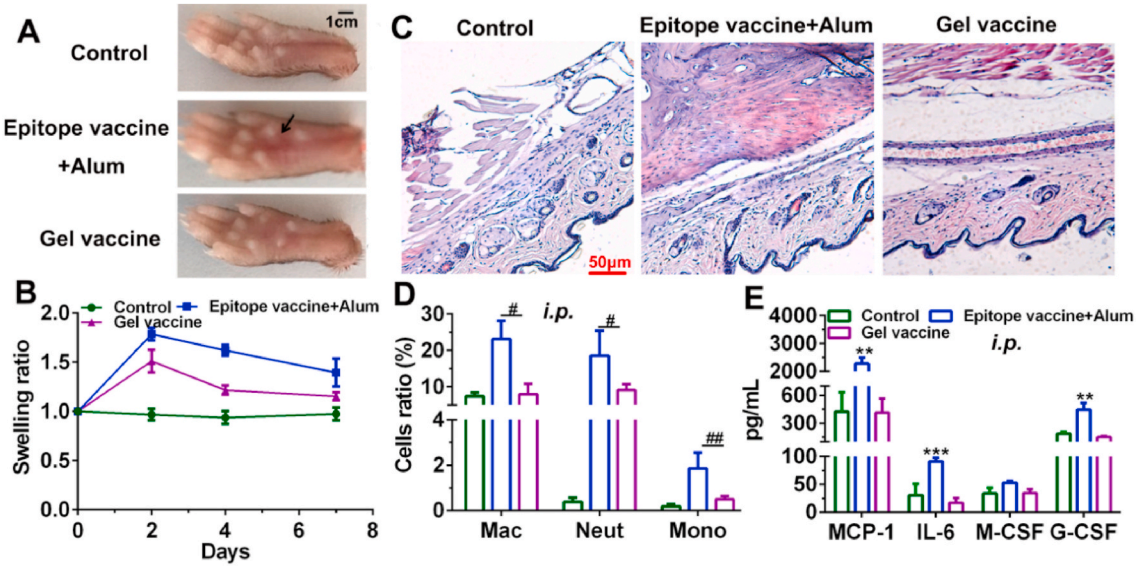

Fig. 4. Co-assembled peptide vaccine did not induce detectable inflammation at the injection location. (A) Representative images of footpads from mice injected with co-assembled K-OVA$_{257\text{-}264}$/E-OVA$_{323\text{-}336}$ hydrogel vaccine or epitope vaccine in Alum. (B) The swelling ratio of footpads after vaccine injection. (C) H&E staining of footpad sections. (D) The recruitment of cells including macrophages (Mac), neutrophils (Neut), and monocytes (Mono), and (E) the secretion of inflammatory cytokines in enterocoelia at 24 h after i.p. injection. Data are shown as mean ± SDs (n = 3). $^{**}P < 0.01$ and $^{***}P < 0.001$, versus the control; $^{\#}P < 0.05$ and $^{\#\#}P < 0.01$, between the indicated groups.

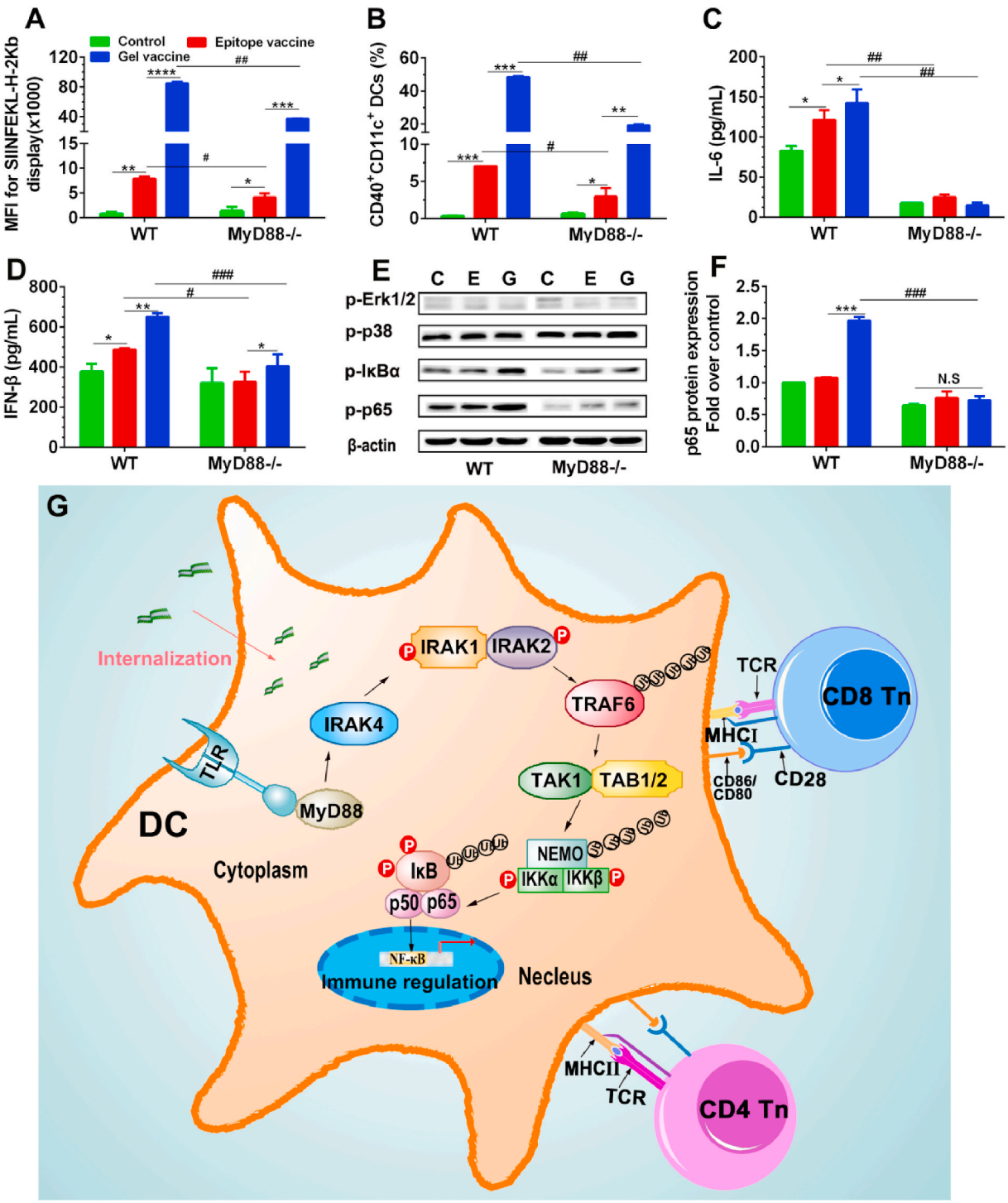

Fig. 5. Co-assembled peptide vaccine activated the MyD88-dependent NF-κB signaling pathway in DCs. (A) Mean fluorescence intensity of SIINFEKL presented by DCs and (B) the ratio of $CD40^{+}CD11c^{+}$ cells detected by flow cytometry. (C, D) The secretion of IL-6 (C) and IFN-β (D) as measured by ELISA. (E) Western blot analysis of the phosphorylation and activation of p38, ERK, IκBα and p65 using β-actin as the loading control. (F) The quantitative analysis of p65. (G) Diagram of NF-κB signal pathway. *, $^{\#}P < 0.05$, **, $^{\#\#}P < 0.01$ and ***, $^{\#\#\#}P < 0.001$, between the indicated groups.

signaling pathway. NF-κB is a key mediator in regulating the innate and adaptive immune responses [60,61], which could promote MHC-I-mediated antigen cross-presentation, upregulate costimulatory molecules, and enhance the expression of pro-inflammatory cytokines. Signaling proteins including p38, Erk1/2, IκBα and p65 were measured by Western blot assay after vaccine stimulation. Fig. 5E and F revealed that co-assembled hydrogel vaccine significantly improved the phosphorylation of IkB-α and p65 in BMDCs from WT mice, in comparison with the stimulation of PBS and free epitope vaccine; however, these proteins were both significantly abolished in MyD88−/− DCs, consistent with the expression of pro-inflammatory cytokine IL-6. Moreover, the phosphorylation of Erk1/2 and P38 were not influenced by the knockout of MyD88. These data demonstrated the immunization of co-assembled peptide vaccine could efficiently activate the NF-κB signaling pathway that required the adaptor protein MyD88. The upstream targets for NF-κB activation remain to be examined in future. The

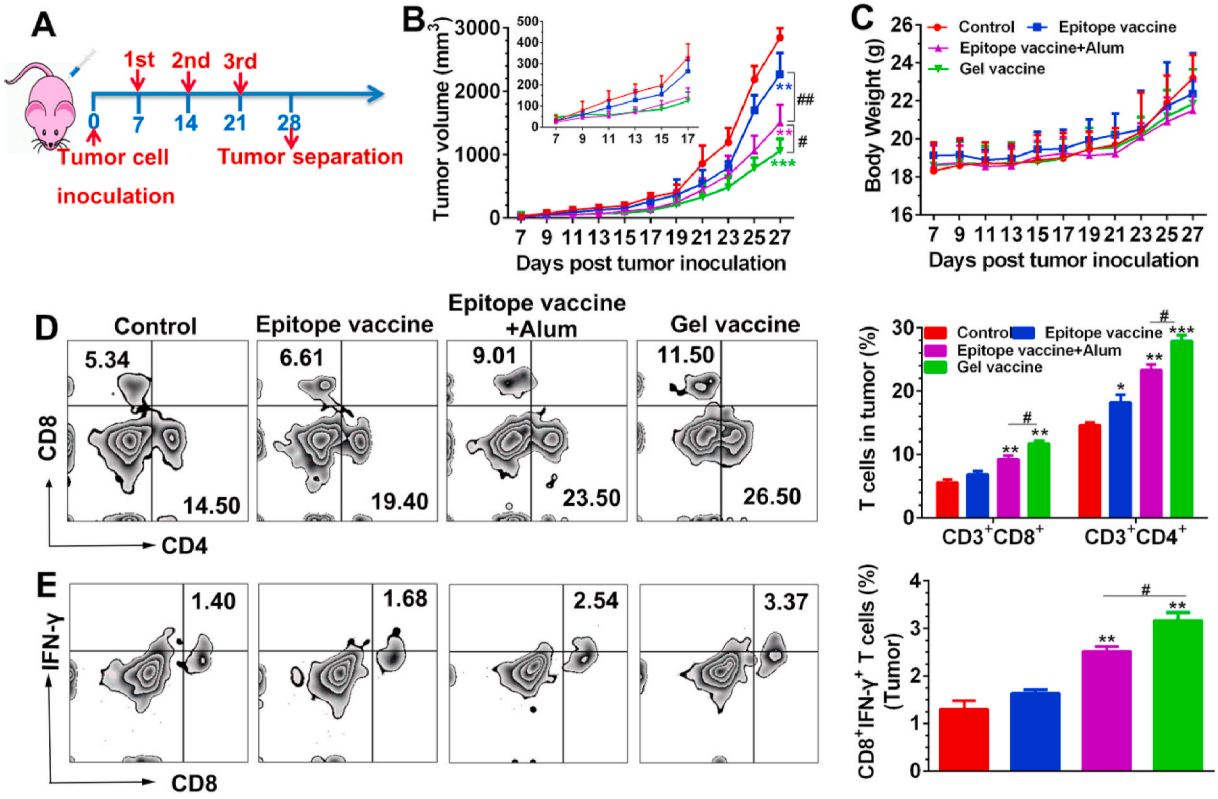

Fig. 6. Co-assembled, self-adjuvanting peptide hydrogel vaccine increased the immunotherapy efficiency against E.G7-OVA lymphoma. (A) The schematic protocol for therapeutic immunotherapy. Epitope vaccine, $OVA_{257-264}$/$OVA_{323-336}$; Gel vaccine, K-$OVA_{257-264}$/E-$OVA_{323-336}$. The mass ratio between two peptides was 1/1. The dose for $OVA_{257-264}$ or $OVA_{323-336}$ was 200 μg/mouse. (B) The curve of tumor volumes. (C) The profile of mice body weight. (D, E) Representative flow cytometry profiles and the percentages of $CD3^+CD8^+$, $CD3^+CD4^+$ (D), and $CD8^+$ IFN-γ^+ (E) T cells infiltrated in tumor. Data represent mean ± SDs (n = 5). $^*P < 0.05$, $^{**}P < 0.01$ and $^{***}P < 0.001$, versus the control; $^{\#}P < 0.05$ and $^{\#\#}P < 0.01$, between the indicated groups.

detailed signaling route in DCs was depicted in Fig. 5G. These results suggested the specific activation of NF-κB pathway in DCs should stimulate the natural pathway of antigen presentation that could modulate the expression of MHC molecules, and the secretion of cytokines and chemokines, which greatly enhanced the adaptive T-cell immune response.

3.5. *Vaccination of co-assembled peptide vaccine improved the therapeutic immunotherapy effect against E.G7-OVA tumor without adjuvants*

Finally, we examined the therapeutic efficiency of co-assembled peptide vaccine in mice that were received s.c. inoculation of 1×10^6 E G7-OVA cells. After 7 days, vaccination was implemented following the protocol illustrated in Fig. 6A. The dose of peptide antigens was 200 μg per mouse. During the entire 28-day experiment period, all mice survived. As shown in Fig. 6B, untreated mice showed rapid tumor growth. The therapeutic vaccination with gel vaccine substantially slowed the tumor growth, which was significantly superior over formulations including peptide vaccine in solution and Alum-adjuvanted vaccine. All treatments did not cause any reduction in animal body weight (Fig. 6C). T-cell subtypes within spleens and tumors were detected to testify the level of antitumor T-cell responses. Fig. 6D shows that the vaccination of peptide hydrogel generated an extensive infiltration of T cells into tumors, providing a nearly 2-fold increase in the ratio of both $CD3^+CD8^+$ and $CD3^+CD4^+$ T cells over control group, which was also significantly higher in comparison with free peptide vaccine and Alum-adjuvanted vaccine. Moreover, in comparison with Alum-adjuvanted epitope vaccine, vaccination of co-assembled peptide hydrogel also obviously augmented the percentage of activated tumor-infiltrating T cells (Fig. 6E), as characterized by the co-expression of IFN-γ, a typical marker for indicating the activation of $CD8^+$ T cells. The frequency of cytotoxic T cells (Fig. S13A, 13B) in spleens was also significantly increased while Tregs ($Foxp3^+$ CD4 T cells, Fig. S13C) was reduced from hydrogel-vaccinated mice, in contrast to other vaccination approaches, indicating the initiation of systemic antitumor T-cell response. These results highlight the great significance of spontaneous co-assembly of ECPs as a self-adjuvanting vaccination strategy to generate a productive response to immunotherapy, which could augment the efficacy of antitumor T-cell immunity against established E.G7-OVA tumors. It should be noticed that no tumor eradication was observed in each vaccine group, indicating the ratio of MHCI-restricted epitope in vaccine needs to be optimized to further improve cytotoxic $CD8^+$ T-cell response in future works. Moreover, tumor immunosuppressive microenvironment should also be inhibited by introducing immune checkpoint blockade such as anti-PD-1 therapy that can specially block the interaction between PD-L1 expressed on tumor cells and PD-1 on effector CD T cells, which would further boost the killing efficiency of effector CD8 T cells infiltrated in tumors. Overall, supramolecular co-assembly of peptides could be adopted as an alternative approach to manufacturing divalent and nanoscale peptide vaccines without the additional use of delivery systems or immunoadjuvants.

4. Conclusions

In summary, we report supramolecular peptide co-assembly as an alternative and robust approach to manufacturing adjuvant-free vaccines with nanostructures. ECPs containing epitopes targeting CD8 or CD4 T-cells could co-assemble into nanofibers or nanoparticles in aqueous solution, irrespective of the physicochemical properties of

antigenic peptides. Significantly, co-assembled peptide vaccine augmented the antigen immunogenicity by increasing antigen cross-presentation in coordination with the activation of NF-κB pathway in DCs that required the adaptor protein MyD88. Co-assembled peptide vaccine resulted in maximized T-cell priming efficiency and a higher breadth of epitope-specific CD8 and CD4 T cells than the free or adjuvant-assistant peptide vaccine. Such a facile and efficient co-assembly strategy is promising for engineering a range of di-/multivalent molecular vaccines by engaging two or multiple peptide epitopes to further broaden the type of antigen-specific T-cell responses. In addition, this vaccine platform may be generally applicable for personalized immunotherapy with neo-epitopes.

Declaration of competing interest

The authors declare no conflict of interest.

CRediT authorship contribution statement

Qi Su: Conceptualization, Methodology, Investigation, Validation, Formal analysis, Writing – original draft. **Huijuan Song:** Methodology, Investigation, Validation, Formal analysis, Funding acquisition, Writing – review & editing. **Pingsheng Huang:** Methodology, Investigation, Validation, Formal analysis, Writing – review & editing. **Chuangnian Zhang:** Methodology, Formal analysis. **Jing Yang:** Validation, Formal analysis. **Deling Kong:** Validation, Formal analysis, Writing – review & editing. **Weiwei Wang:** Conceptualization, Project administration, Funding acquisition, Supervision.

Acknowledgements

This work was financially supported by the National Natural Science Foundation of China (No. 31870950), China Postdoctoral Science Foundation (No. 2019M660029), Non-profit Central Research Institute Fund of Chinese Academy of Medical Sciences (No. 2018RC350017), and Young Elite Scientists Sponsorship Program by Tianjin (TJSQNTJ-2018-01).

Appendix A. Supplementary data

Supplementary data to this article can be found online at https://doi.org/10.1016/j.bioactmat.2021.03.041.

References

[1] C.H. June, R.S. O'Connor, O.U. Kawalekar, S. Ghassemi, M.C. Milone, CAR T cell immunotherapy for human cancer, Science 359 (2018) 1361–1365.
[2] U. Sahin, Ö. Türeci, Personalized vaccines for cancer immunotherapy, Sci. Transl. Med. 359 (2018) 1355–1360.
[3] R.J. Motzer, N.M. Tannir, D.F. McDermott, O. Arén Frontera, B. Melichar, T. K. Choueiri, et al., Nivolumab plus Ipilimumab versus sunitinib in advanced renal-cell carcinoma, N. Engl. J. Med. 378 (2018) 1277–1290.
[4] J.D. Wolchok, H. Kluger, M.K. Callahan, M.A. Postow, N.A. Rizvi, A.M. Lesokhin, et al., Nivolumab plus Ipilimumab in advanced melanoma, N. Engl. J. Med. 369 (2013) 122–133.
[5] D.M. Pardoll, The blockade of immune checkpoints in cancer immunotherapy, Nat. Rev. Canc. 12 (2012) 252–264.
[6] I. Melero, G. Gaudernack, W. Gerritsen, C. Huber, G. Parmiani, S. Scholl, et al., Therapeutic vaccines for cancer: an overview of clinical trials, Nat. Rev. Clin. Oncol. 11 (2014) 509.
[7] U. Sahin, Ö. Türeci, Personalized vaccines for cancer immunotherapy, Science 359 (2018) 1355–1360.
[8] Z. Hu, P.A. Ott, C.J. Wu, Towards personalized, tumour-specific, therapeutic vaccines for cancer, Nat. Rev. Immunol. 18 (2018) 168–182.
[9] N. Hilf, S. Kuttruff-Coqui, K. Frenzel, V. Bukur, S. Stevanović, C. Gouttefangeas, et al., Actively personalized vaccination trial for newly diagnosed glioblastoma, Nature 565 (2019) 240–245.
[10] T.N. Schumacher, R.D. Schreiber, Neoantigens in cancer immunotherapy, Science 348 (2015) 69–74.
[11] P.A. Ott, Z. Hu, D.B. Keskin, S.A. Shukla, J. Sun, D.J. Bozym, et al., An immunogenic personal neoantigen vaccine for patients with melanoma, Nature 547 (2017) 217–221.
[12] M.S. Goldberg, Improving cancer immunotherapy through nanotechnology, Nat. Rev. Canc. 19 (2019) 587–602.
[13] J. Weiden, J. Tel, C.G. Figdor, Synthetic immune niches for cancer immunotherapy, Nat. Rev. Immunol. 18 (2018) 212–218.
[14] R.S. Riley, C.H. June, R. Langer, M.J. Mitchell, Delivery technologies for cancer immunotherapy, Nat. Rev. Drug Discov. 18 (2019) 175–196.
[15] X. He, S.I. Abrams, J.F. Lovell, Peptide delivery systems for cancer vaccines, Advanced Therapeutics (2018) 1800060, 0.
[16] P. Huang, X. Wang, X. Liang, J. Yang, C. Zhang, D. Kong, et al., Nano-, micro-, and macroscale drug delivery systems for cancer immunotherapy, Acta Biomater. 85 (2019) 1–26.
[17] C.B. Fox, J. Haensler, An update on safety and immunogenicity of vaccines containing emulsion-based adjuvants, Expet Rev. Vaccine 12 (2013) 747–758.
[18] E.M. Varypataki, N. Benne, J. Bouwstra, W. Jiskoot, F. Ossendorp, Efficient eradication of established tumors in mice with cationic liposome-based synthetic long-peptide vaccines, Cancer Immunology Research 5 (2017) 222–233.
[19] R. Kuai, L.J. Ochyl, K.S. Bahjat, A. Schwendeman, J.J. Moon, Designer vaccine nanodiscs for personalized cancer immunotherapy, Nat. Mater. 16 (2017) 489–496.
[20] E.A. Scott, A. Stano, M. Gillard, A.C. Maio-Liu, M.A. Swartz, J.A. Hubbell, Dendritic cell activation and T cell priming with adjuvant- and antigen-loaded oxidation-sensitive polymersomes, Biomaterials 33 (2012) 6211–6219.
[21] P. Li, J. Zhou, P. Huang, C. Zhang, W. Wang, C. Li, et al., Self-assembled PEG-b-PDPA-b-PGEM copolymer nanoparticles as protein antigen delivery vehicles to dendritic cells: preparation, characterization and cellular uptake, Regenerative Biomaterials 4 (2017) 11–20.
[22] Q. Ni, F. Zhang, Y. Liu, Z. Wang, G. Yu, B. Liang, et al., A bi-adjuvant nanovaccine that potentiates immunogenicity of neoantigen for combination immunotherapy of colorectal cancer, Science Advances 6 (2020), eaaw6071.
[23] A.W. Li, M.C. Sobral, S. Badrinath, Y. Choi, A. Graveline, A.G. Stafford, et al., A facile approach to enhance antigen response for personalized cancer vaccination, Nat. Mater. 17 (2018) 528–534.
[24] Y. Hailemichael, Z. Dai, N. Jaffarzad, Y. Ye, M.A. Medina, X.-F. Huang, et al., Persistent antigen at vaccination sites induces tumor-specific $CD8^+$ T cell sequestration, dysfunction and deletion, Nat. Med. 19 (2013) 465–472.
[25] G.M. Lynn, C. Sedlik, F. Baharom, Y. Zhu, R.A. Ramirez-Valdez, V.L. Coble, et al., Peptide–TLR-7/8a conjugate vaccines chemically programmed for nanoparticle self-assembly enhance CD8 T-cell immunity to tumor antigens, Nat. Biotechnol. 38 (2020) 320–332.
[26] M. Black, A. Trent, Y. Kostenko, J.S. Lee, C. Olive, M. Tirrell, Self-assembled peptide amphiphile micelles containing a cytotoxic T-cell epitope promote a protective immune response in vivo, Adv. Mater. 24 (2012) 3845–3849.
[27] P. Yang, H. Song, Z. Feng, C. Wang, P. Huang, C. Zhang, et al., Synthetic, supramolecular, and self-adjuvanting $CD8^+$ T-cell epitope vaccine increases the therapeutic antitumor immunity, Advanced Therapeutics 2 (2019) 1900010.
[28] R.R. Pompano, J. Chen, E.A. Verbus, H. Han, A. Fridman, T. McNeely, et al., Titrating T-cell epitopes within self-assembled vaccines optimizes $CD4^+$ helper T cell and antibody outputs, Advanced Healthcare Materials 3 (2014) 1898–1908.
[29] Z.-H. Huang, L. Shi, J.-W. Ma, Z.-Y. Sun, H. Cai, Y.-X. Chen, et al., A totally synthetic, self-assembling, adjuvant-free MUC1 glycopeptide vaccine for cancer therapy, J. Am. Chem. Soc. 134 (2012) 8730–8733.
[30] X. Shi, H. Song, C. Wang, C. Zhang, P. Huang, D. Kong, et al., Co-assembled and self-delivered epitope/CpG nanocomplex vaccine augments peptide immunogenicity for cancer immunotherapy, Chem. Eng. J. 399 (2020) 125854.
[31] H. Liu, K.D. Moynihan, Y. Zheng, G.L. Szeto, A.V. Li, B. Huang, et al., Structure-based programming of lymph-node targeting in molecular vaccines, Nature 507 (2014) 519–522.
[32] E. Alspach, D.M. Lussier, A.P. Miceli, I. Kizhvatov, M. DuPage, A.M. Luoma, et al., MHC-II neoantigens shape tumour immunity and response to immunotherapy, Nature 574 (2019) 696–701.
[33] R. Zander, D. Schauder, G. Xin, C. Nguyen, X. Wu, A. Zajac, et al., $CD4^+$ T cell help is required for the formation of a cytolytic $CD8^+$ T cell subset that protects against chronic infection and cancer, Immunity 51 (2019) 1028–1042.
[34] S. Chen Daniel, I. Mellman, Oncology meets immunology: the cancer-immunity cycle, Immunity 39 (2013) 1–10.
[35] R.A. Fenstermaker, M.J. Ciesielski, J. Qiu, N. Yang, C.L. Frank, K.P. Lee, et al., Clinical study of a survivin long peptide vaccine (SurVaxM) in patients with recurrent malignant glioma, Canc. Immunol. Immunother. 65 (2016) 1339–1352.
[36] C.J.M. Melief, S.H. van der Burg, Immunotherapy of established (pre)malignant disease by synthetic long peptide vaccines, Nat. Rev. Canc. 8 (2008) 351–360.
[37] B. Mukherji, N.G. Chakraborty, S. Yamasaki, T. Okino, H. Yamase, J.R. Sporn, et al., Induction of antigen-specific cytolytic T cells in situ in human melanoma by immunization with synthetic peptide-pulsed autologous antigen presenting cells, Proc. Natl. Acad. Sci. U.S.A. 92 (1995) 8078–8082.
[38] E. Keogh, J. Fikes, S. Southwood, E. Celis, R. Chesnut, A. Sette, Identification of new epitopes from four different tumor-associated antigens: recognition of naturally processed epitopes correlates with HLA-A*0201-binding affinity, J. Immunol. 167 (2001) 787–796.
[39] J. Wang, K. Liu, R. Xing, X. Yan, Peptide self-assembly: thermodynamics and kinetics, Chem. Soc. Rev. 45 (2016) 5589–5604.
[40] C. Yuan, W. Ji, R. Xing, J. Li, E. Gazit, X. Yan, Hierarchically oriented organization in supramolecular peptide crystals, Nature Reviews: Chemistry 3 (2019) 567–588.
[41] C. Yuan, A. Levin, W. Chen, R. Xing, Q. Zou, T.W. Herling, et al., Nucleation and growth of amino acid and peptide supramolecular polymers through liquid–liquid phase separation, Angew. Chem. Int. Ed. 58 (2019) 18116–18123.

[42] Y. Zhang, H. Song, H. Zhang, P. Huang, J. Liu, L. Chu, et al., Fine tuning the assembly and gel behaviors of PEGylated polypeptide conjugates by the copolymerization ofl-alanine and γ-benzyl-l-glutamate N-carboxyanhydrides, J. Polym. Sci. Polym. Chem. 55 (2017) 1512–1523.
[43] M.K. Joo, D.Y. Ko, S.J. Jeong, M.H. Park, U.P. Shinde, B. Jeong, Incorporation of d-alanine into poly(ethylene glycol) and L-poly(alanine-co-phenylalanine) block copolymers affects their nanoassemblies and enzymatic degradation, Soft Matter 9 (2013) 8014–8022.
[44] P. Huang, H. Song, Y. Zhang, J. Liu, Z. Cheng, X.-J. Liang, et al., FRET-enabled monitoring of the thermosensitive nanoscale assembly of polymeric micelles into macroscale hydrogel and sequential cognate micelles release, Biomaterials 145 (2017) 81–91.
[45] S.K. Wculek, F.J. Cueto, A.M. Mujal, I. Melero, M.F. Krummel, D. Sancho, Dendritic cells in cancer immunology and immunotherapy, Nat. Rev. Immunol. 20 (2020) 7–24.
[46] S.K. Saini, K. Ostermeir, V.R. Ramnarayan, H. Schuster, M. Zacharias, S. Springer, Dipeptides promote folding and peptide binding of MHC class I molecules, Proc. Natl. Acad. Sci. U.S.A. 110 (2013) 15383–15388.
[47] S.G. Reed, M.T. Orr, C.B. Fox, Key roles of adjuvants in modern vaccines, Nat. Med. 19 (2013) 1597–1608.
[48] G. Del Giudice, R. Rappuoli, A.M. Didierlaurent, Correlates of adjuvanticity: a review on adjuvants in licensed vaccines, Semin. Immunol. 39 (2018) 14–21.
[49] M. Kool, K. Fierens, B.N. Lambrecht, Alum adjuvant: some of the tricks of the oldest adjuvant, J. Med. Microbiol. 61 (2012) 927–934.
[50] A. Pashine, N.M. Valiante, J.B. Ulmer, Targeting the innate immune response with improved vaccine adjuvants, Nat. Med. 11 (2005) S63–S68.
[51] D.W. Cain, S.E. Sanders, M.M. Cunningham, G. Kelsoe, Disparate adjuvant properties among three formulations of “alum”, Vaccine 31 (2013) 653–660.
[52] J. Chen, R.R. Pompano, F.W. Santiago, L. Maillat, R. Sciammas, T. Sun, et al., The use of self-adjuvanting nanofiber vaccines to elicit high-affinity B cell responses to peptide antigens without inflammation, Biomaterials 34 (2013) 8776–8785.
[53] S.T. Schmidt, S. Khadke, K.S. Korsholm, Y. Perrie, T. Rades, P. Andersen, et al., The administration route is decisive for the ability of the vaccine adjuvant CAF09 to induce antigen-specific CD8+ T-cell responses: the immunological consequences of the biodistribution profile, J. Contr. Release 239 (2016) 107–117.
[54] E. Belnoue, J.-F. Mayol, S. Carboni, W. Di Berardino Besson, E. Dupuychaffray, A. Nelde, et al., Targeting self- and neoepitopes with a modular self-adjuvanting cancer vaccine, JCI Insight 4 (2019), e127305.
[55] H. Cai, M.-S. Chen, Z.-Y. Sun, Y.-F. Zhao, H. Kunz, Y.-M. Li, Self-adjuvanting synthetic antitumor vaccines from MUC1 glycopeptides conjugated to T-cell epitopes from tetanus toxoid, Angew. Chem. Int. Ed. 52 (2013) 6106–6110.
[56] J.S. Rudra, Y.F. Tian, J.P. Jung, J.H. Collier, A self-assembling peptide acting as an immune adjuvant, Proc. Natl. Acad. Sci. U.S.A. 107 (2009) 622–627.
[57] F.A. Sharp, D. Ruane, B. Claass, E. Creagh, J. Harris, P. Malyala, et al., Uptake of particulate vaccine adjuvants by dendritic cells activates the NALP3 inflammasome, Proc. Natl. Acad. Sci. U.S.A. 106 (2009) 870–875.
[58] A. Seubert, S. Calabro, L. Santini, B. Galli, A. Genovese, S. Valentini, et al., Adjuvanticity of the oil-in-water emulsion MF59 is independent of Nlrp3 inflammasome but requires the adaptor protein MyD88, Proc. Natl. Acad. Sci. U.S.A. 108 (2011) 11169–11174.
[59] G.M. Barton, R. Medzhitov, Toll-like receptor signaling pathways, Science 300 (2003) 1524–1525.
[60] G. Bonizzi, M. Karin, The two NF-κB activation pathways and their role in innate and adaptive immunity, Trends Immunol. 25 (2004) 280–288.
[61] K. Taniguchi, M. Karin, NF-κB, inflammation, immunity and cancer: coming of age, Nat. Rev. Immunol. 18 (2018) 309–324.